



FROSCH Preconditioners for Land Ice Simulations of Greenland and Antarctica

Alexander Heinlein¹ Mauro Perego² Sivasankaran Rajamanickam² Ichitaro Yamazaki²

Trilinos User-Developer Group Meeting 2021, 30 November–2 December, 2021

¹Delft University of Technology

²Sandia National Laboratories

Land Ice Simulations of Greenland and Antarctica

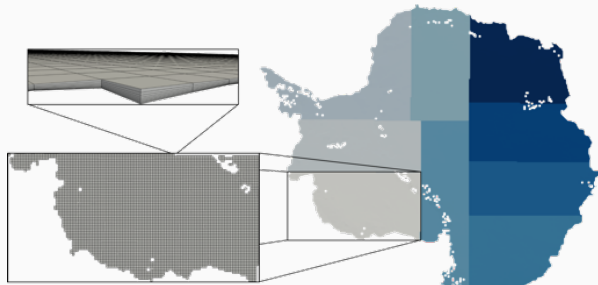
Greenland and Antarctica ice sheets

- store most of the fresh water on earth and
- mass loss from these ice sheets significantly contributes to sea-level rise.

The simulation of **temperature and velocity** of the ice sheets gives rise to **large highly nonlinear systems of equations** with a strong coupling of the variables.



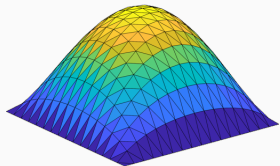
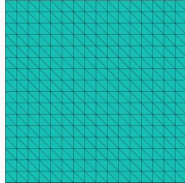
Taken from <https://unsplash.com>



The simulations are also characterized by:

- The **mesh structure**:
 - Volume mesh is obtained by **extrusion** of the surface mesh
⇒ **2D domain decomposition**.
 - **Highly anisotropic**.
- Specific combination of Dirichlet, Neumann, and Robin **boundary conditions**.

Model Problem & Domain Decomposition



Consider a **Poisson model problem** on $[0, 1]^2$:

$$\begin{aligned} -\Delta u &= f \quad \text{in } \Omega, \\ u &= 0 \quad \text{on } \partial\Omega. \end{aligned}$$

Discretize (e.g., using finite elements)

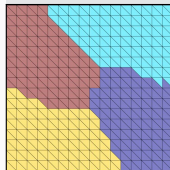
$$Kx = b.$$

⇒ Construct a **parallel scalable**
preconditioner M^{-1} using **overlapping**
Schwarz domain decomposition methods.

Overlapping domain decomposition

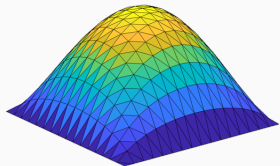
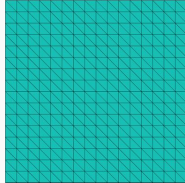
Overlapping Schwarz methods are based on **overlapping decompositions** of the computational domain Ω .

Overlapping subdomains $\Omega'_1, \dots, \Omega'_N$ can be constructed by **recursively adding layers of elements** to nonoverlapping subdomains $\Omega_1, \dots, \Omega_N$.



Nonoverlap. DD

Model Problem & Domain Decomposition



Consider a **Poisson model problem** on $[0, 1]^2$:

$$\begin{aligned} -\Delta u &= f \quad \text{in } \Omega, \\ u &= 0 \quad \text{on } \partial\Omega. \end{aligned}$$

Discretize (e.g., using finite elements)

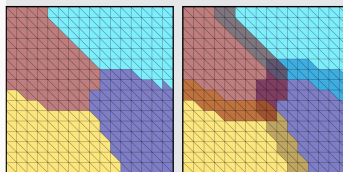
$$Kx = b.$$

⇒ Construct a **parallel scalable**
preconditioner M^{-1} using **overlapping**
Schwarz domain decomposition methods.

Overlapping domain decomposition

Overlapping Schwarz methods are based on **overlapping decompositions** of the computational domain Ω .

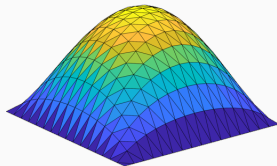
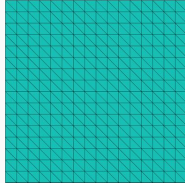
Overlapping subdomains $\Omega'_1, \dots, \Omega'_N$ can be constructed by **recursively adding layers of elements** to nonoverlapping subdomains $\Omega_1, \dots, \Omega_N$.



Nonoverlap. DD

Overlap $\delta = 1h$

Model Problem & Domain Decomposition



Consider a **Poisson model problem** on $[0, 1]^2$:

$$\begin{aligned} -\Delta u &= f \quad \text{in } \Omega, \\ u &= 0 \quad \text{on } \partial\Omega. \end{aligned}$$

Discretize (e.g., using finite elements)

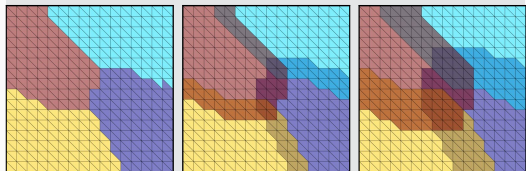
$$Kx = b.$$

⇒ Construct a **parallel scalable**
preconditioner M^{-1} using **overlapping**
Schwarz domain decomposition methods.

Overlapping domain decomposition

Overlapping Schwarz methods are based on **overlapping decompositions** of the computational domain Ω .

Overlapping subdomains $\Omega'_1, \dots, \Omega'_N$ can be constructed by **recursively adding layers of elements** to nonoverlapping subdomains $\Omega_1, \dots, \Omega_N$.



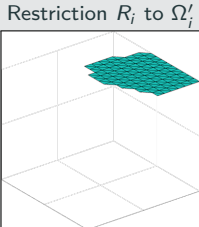
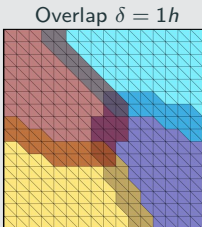
Nonoverlap. DD

Overlap $\delta = 1h$

Overlap $\delta = 2h$

Two-Level Schwarz Preconditioners

One-Level Schwarz preconditioner



Based on an **overlapping domain decomposition**, we define a **one-level Schwarz operator**

$$M_{\text{OS-1}}^{-1} K = \sum_{i=1}^N R_i^T K_i^{-1} R_i K,$$

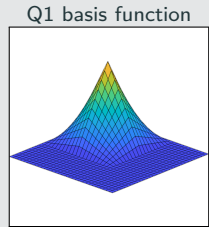
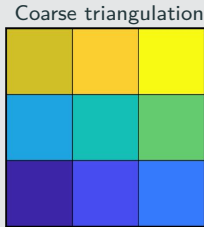
where R_i and R_i^T are restriction and prolongation operators corresponding to Ω'_i , and $K_i := R_i K R_i^T$.
→ **algebraic**

Condition number estimate:

$$\kappa(P_{\text{OS-1}}) \leq C \left(1 + \frac{1}{H\delta} \right)$$

with subdomain size H and the width of the overlap δ .

Adding a Lagrangian coarse space



The **two-level overlapping Schwarz operator** reads

$$M_{\text{OS-2}}^{-1} K = \underbrace{\Phi K_0^{-1} \Phi^T K}_{\text{coarse level - global}} + \underbrace{\sum_{i=1}^N R_i^T K_i^{-1} R_i K}_{\text{first level - local}},$$

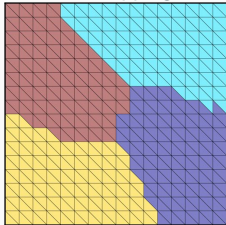
where Φ contains the coarse basis functions and $K_0 := \Phi^T K \Phi$; cf., e.g., [Toselli, Widlund \(2005\)](#).

A Lagrangian coarse basis requires a coarse triangulation (geometric information) → **not algebraic**

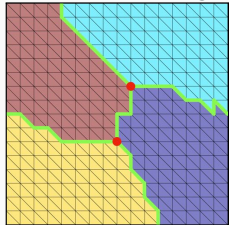
$$\Rightarrow \kappa(P_{\text{OS-2}}) \leq C \left(1 + \frac{H}{\delta} \right)$$

Extension-Based GDSW Coarse Spaces

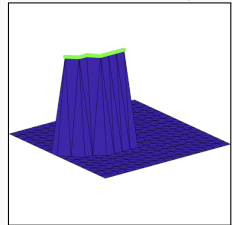
Non-overlapping DD



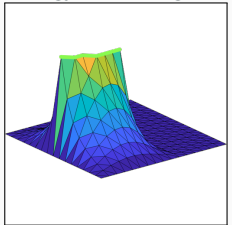
Ident. vertices & edges



Restr. of the null space



Energy minimizing ext.



In **GDSW (Generalized–Dryja–Smith–Widlund)** coarse spaces, the coarse basis functions are chosen as **energy minimizing extensions** of functions Φ_Γ that are defined on the interface Γ :

$$\Phi = \begin{bmatrix} -K_{II}^{-1} K_{\Gamma I}^T \Phi_\Gamma \\ \Phi_\Gamma \end{bmatrix} = \begin{bmatrix} \Phi_I \\ \Phi_\Gamma \end{bmatrix}$$

The functions Φ_Γ are **restrictions of the null space of global Neumann matrix** to the edges, vertices, and, in 3D, faces (**partition of unity**) of the non-overlapping decomposition.

The **condition number of the GDSW operator** is bounded by

$$\kappa(M_{\text{GDSW}}^{-1} K) \leq C \left(1 + \frac{H}{\delta}\right) \left(1 + \log \left(\frac{H}{h}\right)\right)^2;$$

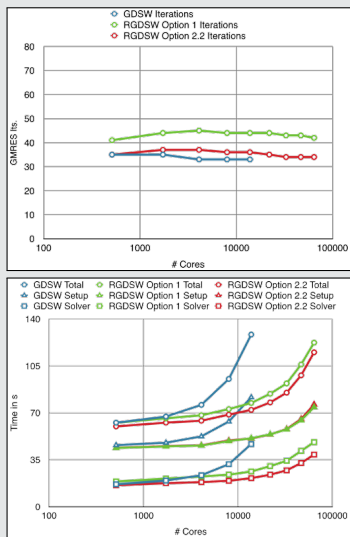
cf. [Dohrmann, Klawonn, Widlund \(2008\)](#), [Dohrmann, Widlund \(2009, 2010, 2012\)](#).

→ We only obtain the exponent 2 for very irregular subdomains.

→ **Scalable and algebraic!**

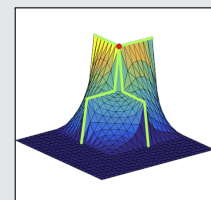
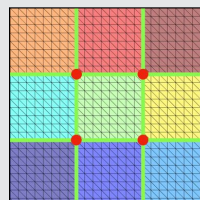
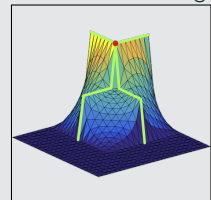
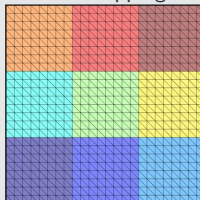
GDSW vs RGDSW (reduced dimension)

Heinlein, Klawonn, Rheinbach, Widlund (2019).



RGDSW (Reduced dimension GDSW)

Non-overlapping DD Ident. vertices & edges



RGDSW option 1

RGDSW option 2.2

Reduced dimension GDSW coarse spaces are constructed from **nodal interface functions (different partition of unity)**; cf. Dohrmann, Widlund (2017).

Software Framework for the Land Ice Simulations



FROSCH (Fast and Robust Overlapping Schwarz) preconditioners through Stratimikos/Thyra interface.



<https://github.com/trilinos/Trilinos>



<https://github.com/SNLComputation/Albany>

Software Framework for the Land Ice Simulations



FROSCh (Fast and Robust Overlapping Schwarz) preconditioners through Stratimikos/Thyra interface.



<https://github.com/trilinos/Trilinos>



<https://github.com/SNLComputation/Albany>

Hardware

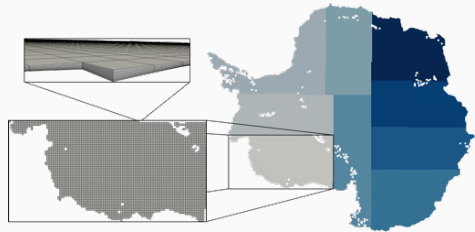
If not mentioned otherwise, the simulations were performed on the Cori supercomputer (NERSC).

Velocity Problem

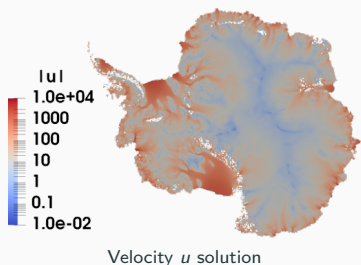
We use a first-order (or Blatter-Pattyn) approximation of the Stokes equations

$$\begin{cases} -\nabla \cdot (2\mu \dot{\epsilon}_1) = -\rho_i |\mathbf{g}| \partial_x s, \\ -\nabla \cdot (2\mu \dot{\epsilon}_2) = -\rho_i |\mathbf{g}| \partial_y s, \end{cases}$$

with the ρ_i the ice density, the ice surface elevation $s(x, y)$, the gravity acceleration \mathbf{g} , and strain rates $\dot{\epsilon}_1$ and $\dot{\epsilon}_2$; cf. [Blatter \(1995\)](#) and [Pattyn \(2003\)](#).



Antarctica mesh & domain decomposition.



Velocity u solution

Nonlinear viscosity model

The ice viscosity μ is modeled using [Glen's law](#)

$$\mu = \frac{1}{2} A(T)^{-\frac{1}{n}} \dot{\epsilon}_e^{\frac{1-n}{n}},$$

where $A(T) = \alpha_1 e^{\alpha_2 T}$ is a temperature-dependent rate factor, $n = 3$ is the power-law exponent, and the effective strain rate $\dot{\epsilon}_e$.

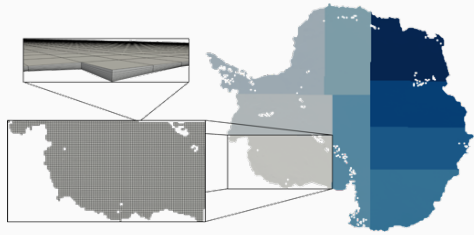
See [Perego, Gunzburger, Burkardt \(2012\)](#) and [Tezaur, Perego, Salinger, Tuminaro, Price \(2015\)](#) for more details.

Velocity Problem

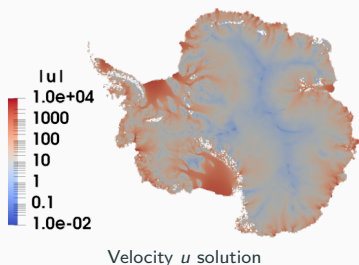
We use a first-order (or Blatter-Pattyn) approximation of the Stokes equations

$$\begin{cases} -\nabla \cdot (2\mu \dot{\epsilon}_1) = -\rho_i |\mathbf{g}| \partial_x s, \\ -\nabla \cdot (2\mu \dot{\epsilon}_2) = -\rho_i |\mathbf{g}| \partial_y s, \end{cases}$$

with the ρ_i the ice density, the ice surface elevation $s(x, y)$, the gravity acceleration \mathbf{g} , and strain rates $\dot{\epsilon}_1$ and $\dot{\epsilon}_2$; cf. [Blatter \(1995\)](#) and [Pattyn \(2003\)](#).



Antarctica mesh & domain decomposition.



Boundary conditions

- *Upper surface:* $\dot{\epsilon}_j = 0, j = 1, 2$
(stress-free Neumann condition)
- *Lower surface:* $2\mu_e \dot{\epsilon}_j \cdot \mathbf{n} + \beta u = 0, j = 1, 2$
(sliding Robin condition with friction coefficient β)
- *Lateral boundary:* $2\mu \dot{\epsilon}_j \cdot \mathbf{n} = \frac{1}{2}gH(\rho_i - \rho_w r^2) n_1, j = 1, 2$
(open-ocean Neumann condition with density of ocean water ρ_w and ratio of submerged ice thickness r)

See [Perego, Gunzburger, Burkardt \(2012\)](#) and [Tezaur, Perego, Salinger, Tuminaro, Price \(2015\)](#) for more details.

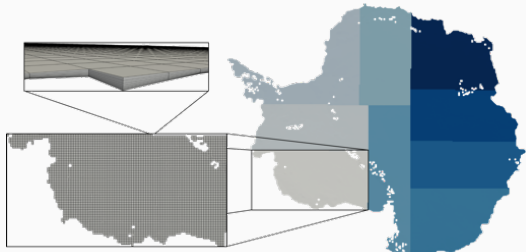
Antarctica Velocity Problem – Comparison of Coarse Spaces (Strong Scaling)

Without rotational coarse basis functions (2 rigid body modes)								
MPI ranks	GDSW				RGDSW			
	dim V_0	avg. its (nl its)	avg. setup	avg. solve	dim V_0	avg. its (nl its)	avg. setup	avg. solve
512	4 598	40.8 (11)	15.36 s	12.38 s	1 834	42.6 (11)	14.99 s	12.50 s
1 024	9 306	43.3 (11)	5.80 s	6.27 s	3 740	44.5 (11)	5.65 s	6.08 s
2 048	18 634	41.7 (11)	3.27 s	2.91 s	7 586	42.7 (11)	3.11 s	2.79 s
4 096	37 184	41.4 (11)	2.59 s	2.07 s	15 324	42.5 (11)	1.07 s	1.54 s
8 192	72 964	39.5 (11)	1.51 s	1.84 s	30 620	42.0 (11)	1.20 s	1.16 s
With rotational coarse basis functions (3 rigid body modes)								
MPI ranks	GDSW				RGDSW			
	dim V_0	avg. its (nl its)	avg. setup	avg. solve	dim V_0	avg. its (nl its)	avg. setup	avg. solve
512	6 897	35.5 (11)	15.77 s	11.21 s	2 751	40.7 (11)	15.23 s	12.22 s
1 024	13 959	35.6 (11)	6.16 s	5.78 s	5 610	42.9 (11)	5.65 s	6.04 s
2 048	27 951	33.5 (11)	3.78 s	3.45 s	11 379	42.2 (11)	3.17 s	2.81 s
4 096	55 776	31.8 (11)	2.21 s	3.80 s	22 986	44.3 (11)	1.95 s	2.70 s
8 192	109 446	29.3 (11)	2.49 s	5.33 s	45 930	40.8 (11)	1.19 s	3.13 s

Problem: Velocity **Mesh:** Antarctica
 4 km hor. resolution
 20 vert. layers **Size:** 35.3 m degrees
 of freedom
 (P1 FE)

Antarctica Velocity Problem – Weak Scalability

- Weak scalability study for an **increasing horizontal mesh resolution**.
 - 1 OpenMP thread:** From 32 to 8 192 processor cores
 - 4 OpenMP threads:** From 128 to 32 768 processor cores
- The **number of vertical layers is fixed to 20**.
- P1 FEM spatial discretization.



Antarctica mesh & domain decomposition.

MPI ranks	mesh	# dofs	1 OpenMP thread			4 OpenMP threads		
			avg. its (nl its)	avg. setup	avg. solve	avg. its (nl its)	avg. setup	avg. solve
32	16 km	2.2 m	24.1 (11)	11.97 s	9.47 s	23.5 (11)	4.15 s	3.25 s
128	8 km	8.8 m	32.0 (10)	14.08 s	8.71 s	32.0 (10)	4.97 s	2.85 s
512	4 km	35.3 m	42.6 (11)	14.99 s	12.50 s	42.6 (11)	5.50 s	4.02 s
2 048	2 km	141.5 m	61.0 (11)	22.83 s	19.76 s	61.0 (11)	7.36 s	6.55 s
8 192	1 km	566.1 m	67.1 (14)	17.36 s	22.91 s	67.1 (14)	6.20 s	7.39 s

Problem: Velocity Meshes: Antarctica 20 vert. layers Discretization: P1 FE Coarse space: RGDSW

Temperature Problem

The steady state enthalpy equation reads

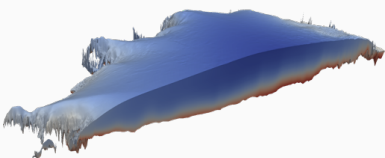
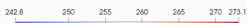
$$\nabla \cdot \mathbf{q}(h) + \mathbf{u} \cdot \nabla h = 4\mu \epsilon_e^2$$

with the enthalpy growing linearly with the water content ϕ

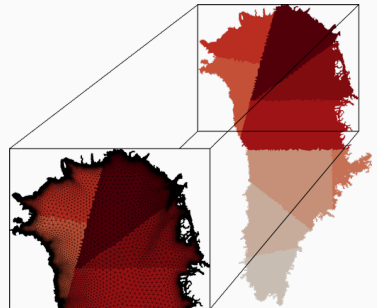
$$h = \begin{cases} \rho_i c (T - T_0), & \text{for cold ice } (h \leq h_m), \\ h_m + \rho_w L \phi, & \text{for temperate ice.} \end{cases}$$

the **melting enthalpy** $h_m := \rho_w c(T_m - T_0)$, the **uniform reference temperature** T_0 , and the **enthalpy flux**

$$\mathbf{q}(h) = \begin{cases} \frac{k}{\rho_i c_i} \nabla h, & \text{for cold ice } (h \leq h_m), \\ \frac{k}{\rho_i c_i} \nabla h_m + \rho_w L \mathbf{j}(h), & \text{for temperate ice.} \end{cases}$$



Temperature T solution



Greenland mesh & domain decomposition.

Water flux term

The water flux term

$$\mathbf{j}(h) := \frac{1}{\eta_w} (\rho_w - \rho_i) k_0 \phi^\gamma \mathbf{g}$$

describes the percolation of water driven by gravity;
cf. [Schoof and Hewitt \(2016, 2017\)](#).

See [Perego et al. \(in preparation\)](#) and [Heinlein et. al \(submitted 2021\)](#) for more details.

Temperature Problem

The steady state enthalpy equation reads

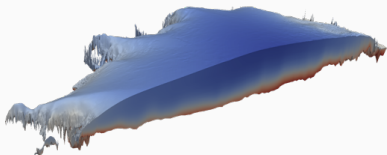
$$\nabla \cdot \mathbf{q}(h) + \mathbf{u} \cdot \nabla h = 4\mu \epsilon_e^2$$

with the enthalpy growing linearly with the water content ϕ

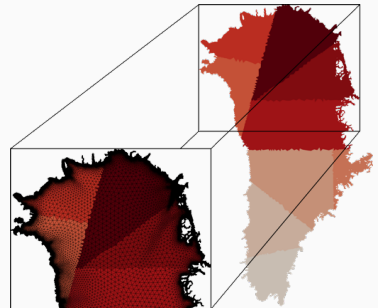
$$h = \begin{cases} \rho_i c (T - T_0), & \text{for cold ice } (h \leq h_m), \\ h_m + \rho_w L \phi, & \text{for temperate ice.} \end{cases}$$

the **melting enthalpy** $h_m := \rho_w c(T_m - T_0)$, the **uniform reference temperature** T_0 , and the **enthalpy flux**

$$\mathbf{q}(h) = \begin{cases} \frac{k}{\rho_i c_i} \nabla h, & \text{for cold ice } (h \leq h_m), \\ \frac{k}{\rho_i c_i} \nabla h_m + \rho_w L \mathbf{j}(h), & \text{for temperate ice.} \end{cases}$$



Temperature T solution



Greenland mesh & domain decomposition.

Boundary conditions

- *Upper surface:* $h = \rho_i c(T_s - T_0)$
(Dirichlet boundary condition)
- *Bed:* $m = G + \beta \sqrt{u^2 + v^2} - k \nabla T \cdot \mathbf{n}$,
 $m(T - T_m) = 0, T_m \leq 0$.
(Stefan boundary condition with melting rate m)

See Perego et al. (in preparation) and Heinlein et. al (submitted 2021) for more details.

Greenland Temperature Problem – One-Level Schwarz VS Two-Level Schwarz

one-level Schwarz preconditioner							
MPI ranks	one layer of algebraic overlap			two layers of algebraic overlap			
	avg. its	avg. setup	avg. solve	avg. its	avg. setup	avg. solve	
512	18.1 (11)	0.42 s	0.35 s	17.1 (11)	0.51 s	0.40 s	
1024	23.7 (11)	0.25 s	0.25 s	22.1 (11)	0.27 s	0.27 s	
2048	29.6 (11)	0.16 s	0.17 s	27.6 (11)	0.23 s	0.20 s	
4096	39.8 (11)	0.15 s	0.15 s	35.6 (11)	0.17 s	0.17 s	

RGDSW preconditioner							
MPI ranks	one layer of algebraic overlap			two layers of algebraic overlap			
	avg. avg. its	avg. setup	avg. solve	avg. avg. its	avg. setup	avg. solve	
512	19.5 (11)	0.44 s	0.41 s	18.7 (11)	0.55 s	0.46 s	
1024	25.2 (11)	0.28 s	0.29 s	23.9 (11)	0.35 s	0.33 s	
2048	31.5 (11)	0.26 s	0.24 s	29.5 (11)	0.25 s	0.27 s	
4096	42.2 (11)	0.25 s	0.27 s	38.2 (11)	0.25 s	0.29 s	

Problem:	Temperature	Mesh:	Greenland 1-10 km hor. resolution 20 vert. layers	Size:	1.9 m degrees of freedom (P1 FE)
-----------------	-------------	--------------	---	--------------	--

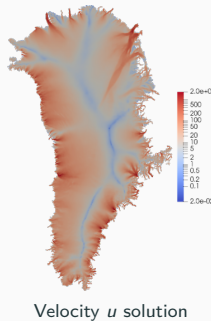
Coupled Problem

Couple the velocity and temperature problems. Therefore, compute the vertical velocity w using the incompressibility condition

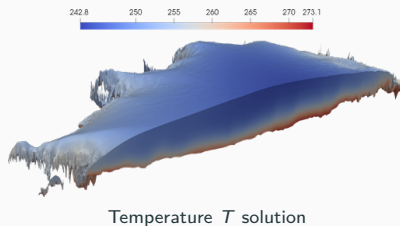
$$\partial_x u + \partial_y v + \partial_z w = 0,$$

with the **Dirichlet boundary condition at the ice lower surface**

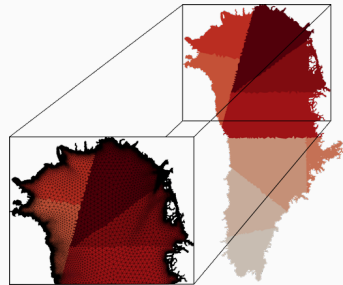
$$\mathbf{u} \cdot \mathbf{n} = \frac{m}{L(\rho_i - \rho_w \phi)}.$$



Velocity u solution



Temperature T solution



Greenland mesh & domain decomposition.

Then, the **tangent matrix** of the coupled problem has the structure

$$\begin{bmatrix} A_u & C_{uT} \\ C_{Tu} & A_T \end{bmatrix} \begin{bmatrix} x_u \\ x_T \end{bmatrix} = \begin{bmatrix} \tilde{r}_u \\ \tilde{r}_T \end{bmatrix}.$$

See [Perego et al. \(in preparation\)](#) and [Heinlein, Perego, Rajamanickam \(submitted 2021\)](#) for more details.

Monolithic (R)GDSW Preconditioners for CFD Simulations

Monolithic GDSW preconditioner

Consider the discrete saddle point problem

$$\mathcal{A}x = \begin{bmatrix} A & B^T \\ B & 0 \end{bmatrix} \begin{bmatrix} u \\ p \end{bmatrix} = \begin{bmatrix} f \\ 0 \end{bmatrix} = b.$$

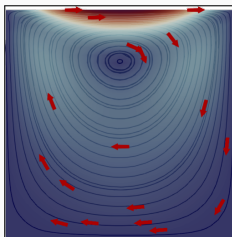
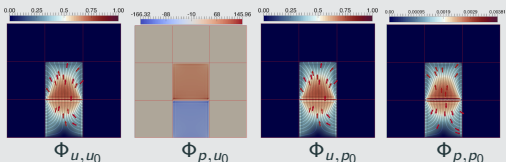
We construct a **monolithic GDSW preconditioner**

$$\mathcal{M}_{\text{GDSW}}^{-1} = \phi \mathcal{A}_0^{-1} \phi^T + \sum_{i=1}^N \mathcal{R}_i^T \mathcal{A}_i^{-1} \mathcal{R}_i,$$

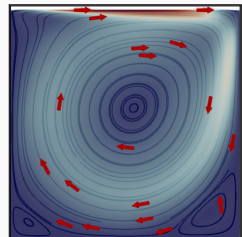
with block matrices $\mathcal{A}_0 = \phi^T \mathcal{A} \phi$, $\mathcal{A}_i = \mathcal{R}_i \mathcal{A} \mathcal{R}_i^T$, and

$$\mathcal{R}_i = \begin{bmatrix} \mathcal{R}_{u,i} & 0 \\ 0 & \mathcal{R}_{p,i} \end{bmatrix} \quad \text{and} \quad \phi = \begin{bmatrix} \Phi_{u,u_0} & \Phi_{u,p_0} \\ \Phi_{p,u_0} & \Phi_{p,p_0} \end{bmatrix}.$$

Using \mathcal{A} to compute extensions: $\phi_I = -\mathcal{A}_{II}^{-1} \mathcal{A}_{I\Gamma} \phi_\Gamma$; cf. [Heinlein, Hochmuth, Klawonn \(2019, 2020\)](#).



Stokes flow



Navier–Stokes flow

Related work:

- Original work on monolithic Schwarz preconditioners: [Klawonn and Pavarino \(1998, 2000\)](#)
- Other publications on monolithic Schwarz preconditioners: e.g., [Hwang and Cai \(2006\)](#), [Barker and Cai \(2010\)](#), [Wu and Cai \(2014\)](#), and the presentation [Dohrmann \(2010\)](#) at the *Workshop on Adaptive Finite Elements and Domain Decomposition Methods* in Milan.

Monolithic (R)GDSW Preconditioners for CFD Simulations

Monolithic GDSW preconditioner

Consider the discrete saddle point problem

$$\mathcal{A}x = \begin{bmatrix} A & B^T \\ B & 0 \end{bmatrix} \begin{bmatrix} u \\ p \end{bmatrix} = \begin{bmatrix} f \\ 0 \end{bmatrix} = b.$$

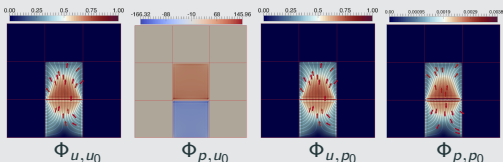
We construct a **monolithic GDSW preconditioner**

$$\mathcal{M}_{\text{GDSW}}^{-1} = \phi \mathcal{A}_0^{-1} \phi^T + \sum_{i=1}^N \mathcal{R}_i^T \mathcal{A}_i^{-1} \mathcal{R}_i,$$

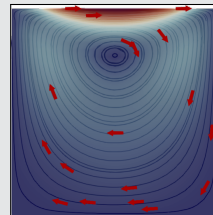
with block matrices $\mathcal{A}_0 = \phi^T \mathcal{A} \phi$, $\mathcal{A}_i = \mathcal{R}_i \mathcal{A} \mathcal{R}_i^T$, and

$$\mathcal{R}_i = \begin{bmatrix} \mathcal{R}_{u,i} & 0 \\ 0 & \mathcal{R}_{p,i} \end{bmatrix} \quad \text{and} \quad \phi = \begin{bmatrix} \Phi_{u,u_0} & \Phi_{u,p_0} \\ \Phi_{p,u_0} & \Phi_{p,p_0} \end{bmatrix}.$$

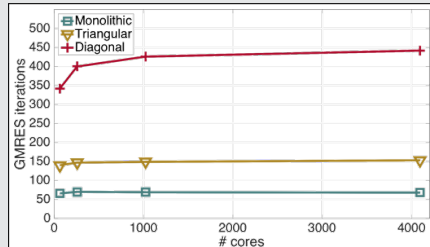
Using \mathcal{A} to compute extensions: $\phi_I = -\mathcal{A}_{II}^{-1} \mathcal{A}_{I\Gamma} \phi_\Gamma$; cf. [Heinlein, Hochmuth, Klawonn \(2019, 2020\)](#).



Monolithic vs Block Preconditioners



Stokes flow



Computations performed on magnitUDE, University Duisburg-Essen.

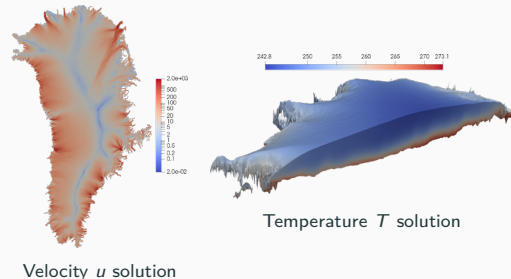
Monolithic (R)GDSW Preconditioners for Multiphysics Land Ice Simulations

We construct a **monolithic two-level (R)GDSW preconditioner** ([Heinlein, Hochmuth, Klawonn \(2019, 2020\)](#))

$$\mathcal{M}_{\text{GDSW}}^{-1} = \phi \mathcal{A}_0^{-1} \phi^T + \sum_{i=1}^N \mathcal{R}_i^T \mathcal{A}_i^{-1} \mathcal{R}_i,$$

for the tangent matrix of the coupled problem

$$\mathcal{A}x := \begin{bmatrix} A_u & C_{uT} \\ C_{Tu} & A_T \end{bmatrix} \begin{bmatrix} x_u \\ x_T \end{bmatrix} = \begin{bmatrix} \tilde{r}_u \\ \tilde{r}_T \end{bmatrix} =: r.$$



Null space

We use an **equal-order P1 finite element discretization in space** for all variables. Therefore, the **null space** in each finite element node is spanned by:

$$r_{u,1} := \begin{bmatrix} 1 \\ 0 \\ 0 \\ 0 \end{bmatrix}, \quad r_{u,2} := \begin{bmatrix} 0 \\ 1 \\ 0 \\ 0 \end{bmatrix}, \quad r_{u,3} := \begin{bmatrix} 0 \\ 0 \\ 1 \\ 0 \end{bmatrix}, \quad r_{u,4} := \begin{bmatrix} y \\ -x \\ 0 \\ 0 \end{bmatrix}, \quad \text{and} \quad r_T := \begin{bmatrix} 0 \\ 0 \\ 0 \\ 1 \end{bmatrix}.$$

See [Heinlein, Perego, Rajamanickam \(submitted 2021\)](#) for more details.

Monolithic (R)GDSW Preconditioners for Multiphysics Land Ice Simulations

We construct a **monolithic two-level (R)GDSW preconditioner** ([Heinlein, Hochmuth, Klawonn \(2019, 2020\)](#))

$$\mathcal{M}_{\text{GDSW}}^{-1} = \phi \mathcal{A}_0^{-1} \phi^T + \sum_{i=1}^N \mathcal{R}_i^T \mathcal{A}_i^{-1} \mathcal{R}_i,$$

for the tangent matrix of the coupled problem

$$\mathcal{A}x := \begin{bmatrix} A_u & C_{uT} \\ C_{Tu} & A_T \end{bmatrix} \begin{bmatrix} x_u \\ x_T \end{bmatrix} = \begin{bmatrix} \tilde{r}_u \\ \tilde{r}_T \end{bmatrix} =: r.$$

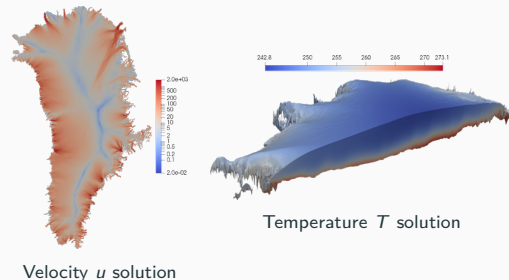
Fully coupled extensions

We compute coarse basis function using extensions

$$\phi = \begin{bmatrix} -\mathcal{A}_{II}^{-1} \mathcal{A}_{\Gamma I}^T \Phi_{\Gamma} \\ \Phi_{\Gamma} \end{bmatrix} = \begin{bmatrix} \phi_I \\ \phi_{\Gamma} \end{bmatrix}$$

based on the coupled matrix \mathcal{A} .

See [Heinlein, Perego, Rajamanickam \(submitted 2021\)](#) for more details.



Decoupled extensions

We compute coarse basis function using extensions

$$\phi = \begin{bmatrix} -\tilde{\mathcal{A}}_{II}^{-1} \tilde{\mathcal{A}}_{\Gamma I}^T \Phi_{\Gamma} \\ \Phi_{\Gamma} \end{bmatrix} = \begin{bmatrix} \phi_I \\ \phi_{\Gamma} \end{bmatrix}$$

based on the decoupled matrix

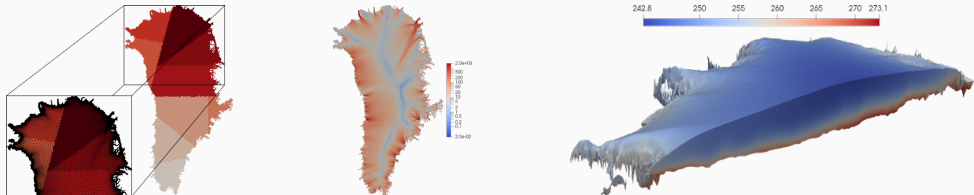
$$\tilde{\mathcal{A}} = \begin{bmatrix} A_u & 0 \\ 0 & A_T \end{bmatrix}.$$

Greenland Coupled Problem – Coarse Spaces

fully coupled extensions							
MPI ranks	dim V_0	no reuse			reuse coarse basis		
		avg. its (nl its)	avg. setup	avg. solve	avg. its (nl its)	avg. setup	avg. solve
256	1 400	100.1 (27)	4.10 s	6.40 s	18.5 (70)	2.28 s	1.07 s
512	2 852	129.1 (28)	1.88 s	4.20 s	24.6 (38)	1.04 s	0.70 s
1 024	6 036	191.2 (65)	1.21 s	4.76 s	34.2 (32)	0.66 s	0.70 s
2 048	12 368	237.4 (30)	0.96 s	4.06 s	37.3 (30)	0.60 s	0.58 s
decoupled extensions							
MPI ranks	dim V_0	no reuse			reuse coarse basis		
		avg. its (nl its)	avg. setup	avg. solve	avg. its (nl its)	avg. setup	avg. solve
256	1 400	23.6 (29)	3.90 s	1.32 s	21.5 (34)	2.23 s	1.18 s
512	2 852	27.5 (30)	1.83 s	0.78 s	26.4 (33)	1.13 s	0.78 s
1 024	6 036	30.1 (29)	1.19 s	0.60 s	28.6 (43)	0.66 s	0.61 s
2 048	12 368	36.4 (30)	0.69 s	0.56 s	31.2 (50)	0.57 s	0.55 s

Problem: Coupled Mesh: Greenland Size: 7.5 m degrees of freedom Coarse space: RGDSW
 Mesh: 3-30 km hor. resolution 20 vert. layers Coarse space: (P1 FE)

Greenland Coupled Problem – Large Problem



MPI ranks	decoupled (no reuse)			fully coupled (reuse coarse basis)			decoupled (reuse 1st level symb. fact. + coarse basis)		
	avg. its. (nl its)	avg. setup	avg. solve	avg. its (nl its)	avg. setup	avg. solve	avg. its (nl its)	avg. setup	avg. solve
512	41.3 (36)	18.78 s	4.99 s	45.3 (32)	11.84 s	5.35 s	45.0 (35)	10.53 s	5.36 s
1 024	53.0 (29)	8.68 s	4.22 s	47.8 (37)	5.36 s	3.82 s	54.3 (32)	4.59 s	4.31 s
2 048	62.2 (86)	4.47 s	4.23 s	66.7 (38)	2.81 s	4.53 s	59.1 (38)	2.32 s	3.99 s
4 096	68.9 (40)	2.52 s	2.86 s	79.1 (36)	1.61 s	3.30 s	78.7 (38)	1.37 s	3.30 s

Problem: Coupled **Mesh:** Greenland
1-10 km hor. resolution
20 vert. layers **Size:** 68.6 m degrees
of freedom
(P1 FE) **Coarse space:** RGDSW

Sparse Triangular Solver in Kokkos-Kernels (Amesos2 – SuperLU/Cholmod)

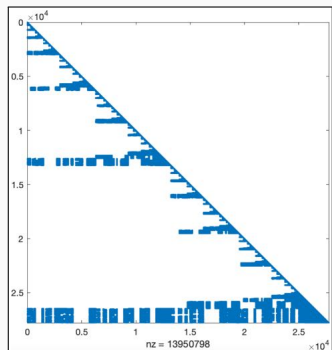
The sparse triangular solver is an **important kernel** in many codes (including FROSch) but is **challenging to parallelize**

- Factorization using a **sparse direct solver** typically leads to triangular matrices with **dense blocks** called **supernodes**
- In **supernodal triangular solver**, rows/columns with a similar sparsity pattern are merged into a supernodal block, and the **solve** is then performed **block-wise**
- The **parallelization potential** for the triangular solver is **determined by the sparsity pattern**

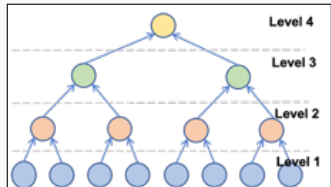
Parallel supernode-based triangular solver:

1. **Supernode-based level-set scheduling**, where **all leaf-supernodes within one level are solved in parallel** (batched kernels for hierarchical parallelism)
2. **Partitioned inverse** of the submatrix associated with each level: **SpTRSV is transformed into a sequence of SpMVs**

See [Yamazaki, Rajamanickam, Ellingwood \(2020\)](#) for more details.



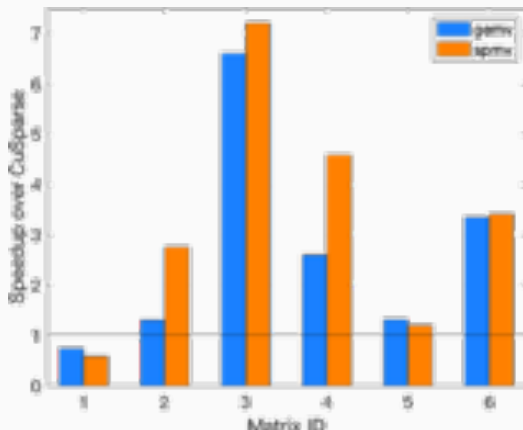
Lower-triangular matrix – SuperLU
with METIS nested dissection ordering



Performance Results With Matrices From the SuiteSparse Matrix Collection

Comparison of the sparse-triangular solve in GEMV and SpMV mode for the matrix vector multiplications against CuSparse sparse triangular solver.

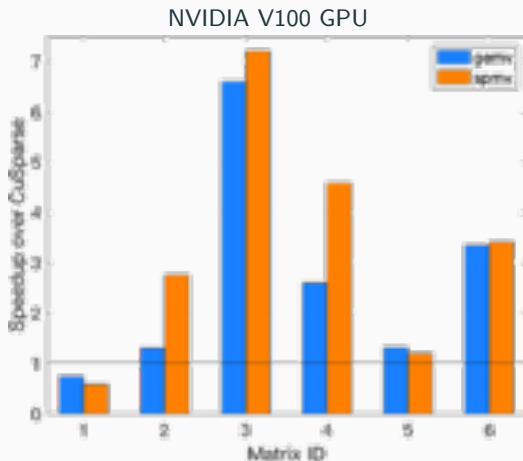
NVIDIA V100 GPU



id	name	type	n	$\frac{n_{nz}}{n}$	n_ℓ	error
1	ACTIVSg70K	power system grid	69,999	12.6	83	0.003
2	dawson5	structural problem	51,537	770.4	1277	3.512
3	qa8fk	acoustic problem	66,127	653.3	22	0.006
4	FEM3Dtherm	thermal problem	17,880	324.6	15	0.008
5	thermal1	thermal problem	82,654	58.7	27	0.002
6	apache1	3D finite difference	80,800	240.2	25	0.002
7	apache2	3D finite difference	715,176	53.6	32	0.001
8	helm2d03	2D problem	392,257	14.9	109	0.018

Performance Results With Matrices From the SuiteSparse Matrix Collection

Comparison of the sparse-triangular solve in GEMV and SpMV mode for the matrix vector multiplications against CuSparse sparse triangular solver.



id	name	type	n	$\frac{n_{nz}}{n}$	n_ℓ	error
1	ACTIVSg70K	power system grid	69,999	12.6	83	0.003
2	dawson5	structural problem	51,537	770.4	1277	3.512
3	qa8fk	acoustic problem	66,127	653.3	22	0.006
4	FEM3Dtherm	thermal problem	17,880	324.6	15	0.008
5	thermal1	thermal problem	82,654	58.7	27	0.002
6	apache1	3D finite difference	80,800	240.2	25	0.002
7	apache2	3D finite difference	715,176	53.6	32	0.001
8	helm2d03	2D problem	392,257	14.9	109	0.018

→ Performance depends on **number of levels** and **sizes of supernodes**.

Preliminary Strong Scaling Results

Computations on Summit (ORNL); $6 \times$ NVIDIA V100 GPUs and $2 \times$ 21-core Power9 per node

		42 MPI ranks per node	6 MPI ranks, 6 GPUs per node	12 MPI ranks, 6 GPUs per node	42 MPI ranks, 6 GPUs per node
1 node	its (nl its)	171			
	subd. setup time	42	506.7 s	6	OOM
	solve time		29.3 s		
2 node	its (nl its)	200 (9)		156 (9)	165 (9)
	subd. setup time	96	165.9 s	12	884.8 s
	solve time		15.3 s	5.9 s	5.3 s
3 node	its (nl its)	208 (9)		178 (9)	180 (9)
	subd. setup time	126	88.1 s	18	506.3 s
	solve time		9.7 s	4.0 s	3.7 s
4 node	its (nl its)	217 (9)		165 (9)	197 (9)
	subd. setup time	168	49.0 s	24	307.7 s
	solve time		7.0 s	3.2 s	3.3 s

Problem: Coupled Mesh: Greenland (structured)
16 km hor. resolution
20 vert. layers Size: 2.0 m degrees of freedom
(P1 FE) Prec.: One-level Schwarz with alg. overlap 0

Preliminary Strong Scaling Results

Computations on Summit (ORNL); $6 \times$ NVIDIA V100 GPUs and $2 \times$ 21-core Power9 per node

		42 MPI ranks per node	6 MPI ranks, 6 GPUs per node	12 MPI ranks, 6 GPUs per node	42 MPI ranks, 6 GPUs per node
1 node	its (nl its)	171			
	subd. setup time	42	506.7 s	6	OOM
	solve time		29.3 s		
2 node	its (nl its)	200 (9)		156 (9)	
	subd. setup time	96	165.9 s	12	2892.7 s
	solve time		15.3 s		5.9 s
3 node	its (nl its)	208 (9)		178 (9)	
	subd. setup time	126	88.1 s	18	1485.3 s
	solve time		9.7 s		4.0 s
4 node	its (nl its)	217 (9)		165 (9)	
	subd. setup time	168	49.0 s	24	848.0 s
	solve time		7.0 s		3.2 s

Problem: Coupled **Mesh:** Greenland (structured)
16 km hor. resolution
20 vert. layers **Size:** 2.0 m degrees
of freedom (P1 FE) **Prec.:** One-level
Schwarz with alg. overlap 0

- Generally, **higher setup times** for the GPU configurations

Preliminary Strong Scaling Results

Computations on Summit (ORNL); $6 \times$ NVIDIA V100 GPUs and $2 \times$ 21-core Power9 per node

		42 MPI ranks per node	6 MPI ranks, 6 GPUs per node	12 MPI ranks, 6 GPUs per node	42 MPI ranks, 6 GPUs per node
1 node	its (nl its)	171			
	subd. setup time	42	506.7 s	6	OOM
	solve time		29.3 s		
2 node	its (nl its)	200 (9)		156 (9)	
	subd. setup time	96	165.9 s	12	2892.7 s
	solve time		15.3 s		5.9 s
3 node	its (nl its)	208 (9)		178 (9)	
	subd. setup time	126	88.1 s	18	1485.3 s
	solve time		9.7 s		4.0 s
4 node	its (nl its)	217 (9)		165 (9)	
	subd. setup time	168	49.0 s	24	848.0 s
	solve time		7.0 s		3.2 s

Problem: Coupled Mesh: Greenland (structured)
16 km hor. resolution
20 vert. layers Size: 2.0 m degrees of freedom
(P1 FE) Prec.: One-level Schwarz with alg. overlap 0

- Generally, **higher setup times** for the GPU configurations
- For many configurations, we obtain a significant **speedup in the solve times**

Preliminary Strong Scaling Results

Computations on Summit (ORNL); $6 \times$ NVIDIA V100 GPUs and $2 \times$ 21-core Power9 per node

		42 MPI ranks per node	6 MPI ranks, 6 GPUs per node	12 MPI ranks, 6 GPUs per node	42 MPI ranks, 6 GPUs per node
1 node	its (nl its)	171			
	subd. setup time	42	506.7 s	6	OOM
	solve time		29.3 s		
2 node	its (nl its)	200 (9)		156 (9)	
	subd. setup time	96	165.9 s	12	2892.7 s
	solve time		15.3 s		5.9 s
3 node	its (nl its)	208 (9)		178 (9)	
	subd. setup time	126	88.1 s	18	1485.3 s
	solve time		9.7 s		4.0 s
4 node	its (nl its)	217 (9)		165 (9)	
	subd. setup time	168	49.0 s	24	848.0 s
	solve time		7.0 s		3.2 s

Problem: Coupled Mesh: Greenland (structured)
16 km hor. resolution
20 vert. layers Size: 2.0 m degrees of freedom
(P1 FE) Prec.: One-level Schwarz with alg. overlap 0

- Generally, **higher setup times** for the GPU configurations
 - For many configurations, we obtain a significant **speedup in the solve times**
- **Removing UVM dependency** and **better parallelization** on the GPUs: **MPS** and **SuperLU_DIST**

Thank you for your attention!

Summary

- Scalable FROSCh preconditioners
 - for the single physics **velocity and temperature problems** and
 - for the **coupled multi physics problem (monolithic (R)GDSW preconditioners)**.
- Preliminary results on GPUs using **parallel sparse triangular solver**.

Outlook

- Improving the robustness of the nonlinear convergence.
- Improving the setup times on GPUs.

Acknowledgements

- **Financial support:** DFG (KL2094/3-1, RH122/4-1), DOE (SciDAC projects FASTMath, ProSPect)
- **Computing resources:** Cori (NERSC), JUQUEEN (JSC), magnitUDE (UDE), Summit (ORNL)

Disclaimer:

SAND2021-15131 C

This presentation describes objective technical results and analysis. Any subjective views or opinions that might be expressed in the paper do not necessarily represent the views of the U.S. Department of Energy or the United States Government.

Sandia National Laboratories is a multimission laboratory managed and operated by National Technology and Engineering Solutions of Sandia, LLC., a wholly owned subsidiary of Honeywell International, Inc., for the U.S. Department of Energy's National Nuclear Security Administration under contract DE-NA-0003525.